

A new quantum machine learning algorithm: split hidden quantum Markov model inspired by quantum conditional master equation

Xiao-Yu Li¹, Qin-Sheng Zhu², Yong Hu², Hao Wu², Guo-Wu Yang³, Lian-Hui Yu², and Geng Chen³

¹School of Information and Software Engineering, University of Electronic Science and Technology of China, Cheng Du, 610054, China

²School of Physics, University of Electronic Science and Technology of China, Cheng Du, 610054, China

³School of Computer Science and Engineering, University of Electronic Science and Technology of China, Cheng Du, 610054, China

The Hidden Quantum Markov Model (HQMM) has significant potential for analyzing time-series data and studying stochastic processes in the quantum domain due to its greater accuracy and efficiency than the classical hidden Markov model. In this work, we introduced the split HQMM (SHQMM) for implementing the hidden quantum Markov process, utilizing the conditional master equation with a fine balance condition to demonstrate the interconnections among the internal states of the quantum system. The experimental results suggest that our model outperforms previous models in terms of performance and robustness. Additionally, we establish a new learning algorithm to solve parameters in HQMM by relating the quantum conditional master equation to the HQMM. Finally, our study provides clear evidence that the quantum transport system can be considered a physical representation of HQMM. The SHQMM with accompanying algorithms present a novel method to analyze quantum systems and time series grounded in physical implementation.

1 Introduction

The significant increase of data and information has emphasized that classical algorithms have difficulties in meeting computation demands for ef-

Qin-Sheng Zhu: Corresponding:zhuqinsheng@uestc.edu.cn

ficiency and speed. Therefore, quantum computing, capable of efficient computation, has become a viable solution. Unlike classical computing, quantum computing employs quantum bits' superposition for data storage, reading, and Efficient computing. As a result, quantum computing promises to solve problems that are too complex for classical computers. Quantum computing originated from Benioff's [1] quantum Turing machine and Feynman's [2] bypassing the difficulty of simulating quantum mechanics with classical computers.

Quantum computing has made great improvements in hardware implementations [3, 4, 5] and algorithmic approaches [6, 7] in the last decade. These advances have propelled the field of quantum computing into the "*Noisy intermediate-scale quantum (NISQ) algorithms*" era. During that era, many hybrid framework [8] algorithms emerged that combined quantum and classical approaches to cope with suboptimal hardware conditions. Initial applications of quantum computing in chemistry [9], Hamiltonian simulation [10], biology [11], pharmaceutical [12], finance [13], materials [14] and various other fields demonstrate its potential advantages over classical computing.

In the field of machine learning, the Hidden Markov Model (HMM) algorithm plays a vitall role and has been extensively and effectively utilized in domains such as stock market forecasting [15, 16], natural language processing [17, 18], protein sequencing [19, 20].

The classical HMM [21] has three main parts: training, decoding, and learning. When the di-

mensionality of the hidden state is not large, the Baum-Welch algorithm [22], the Viterbi algorithm [23], and the EM algorithm [24] can be used to solve these problems efficiently. However, when the dimensions of the hidden state and the observation space increase simultaneously, the solution speed and accuracy of the classical algorithms become weak.

Quantum algorithms were introduced in response to address such problems and find more effective solutions. Monras *et.al.* [25] proposed using random quantum operators to measure an open quantum system, and defined the result of such a random process as the HQMM, and gave the mathematical definition of the hidden quantum Markov process in terms of Kraus operators. This work offers insight into HQMM and a method for studying this model from the perspective of quantum open systems, as well as creating heuristic quantum computing algorithms.

Compared to the classical HMM, the quantum version also functions as a stochastic probability graph model, and it entails the same three main parts. Crucially, solving the model parameters, commonly referred to as the "*learning problem*", is the key to addressing these issues and have series of previous work.

Srinivasan *et. al.*[26] proposed an algorithm based on the Norm Observable Operator Model's learning algorithm, originally presented by Jaeger *et.al.*[27]. This study demonstrates that HQMM offers advantages over traditional algorithms with regard to model complexity and accuracy. Nevertheless, this model is only suitable for situations where the hidden state dimension is relatively small, and it is inclined to succumb to local optimal solutions.

Subsequently, Liu *et.al.* [28] analytically demonstrated the superiority of the quantum stochastic model in comparison to the classical model, providing qualitative evidence that HQMM has advantages over HMM. In 2020, Adhikary *et.al.* [29] proposed a learning algorithm grounded in optimization theory on the manifold [30] with the aim of resolving the Kraus. Our research builds on the foundation laid out by previous work on HQMM. We utilize the conditional master equation with fine balance conditions to analyze the intricate connections within the quantum system and present SHQMM with supporting parameters solve methods.

Motivation

- Our research diverges from previous studies as we approach the HQMM from a physical standpoint, concerning an open quantum system described by the quantum master equation. We developed a new HQMM learning algorithm using the quantum conditional master equation [31, 32, 33], namely SHQMM, which offer a comprehension of the quantum state of the system in fine balance conditions while guaranteeing algorithmic performance.
- Since all quantum algorithms are ultimately executed on physical devices or systems, understanding the physical process behind a quantum algorithm's design not only enhances its interpretability [34], but also facilitates quantum circuit design. Quantum transport systems [35] provide a physical example of the quantum condition master equation, thus serving as a fundamental basis for physical implementation. Combined with Quantum transport systems, we develop SHQMM algorithm that is more practical for applications. Additionally, we have discerned similarities between the model structure and quantum neural network (QNN). Our work is expected to provide new ideas for the physical implementation of QNN.
- Due to its connection to the quantum conditional master equation, HQMM has the capability to function with open systems and non-unitary quantum algorithms, rendering it applicable to the noise-related issues that arise in quantum computers during NISQ.

Main work In this paper, we present a novel HQMM constructed using quantum conditional master equations, building upon the research of Clark et al. [36] Additionally, we introduce a fresh approach to address the challenges of parameter updating and learning. We conduct numerical experiments on both quantum and classical datasets to evaluate the model's performance. The paper is organized as follows: Sec. 2 provides an introduction to the fundamental concepts of HMM and HQMM. Sec. 3 delves into the theoretical aspects of quantum conditional master equation. In Sec. 4, we formally

introduce the Split Hidden Quantum Markov Model (SHQMM), a novel stochastic probabilistic graphical model that incorporates the quantum master equation. The implementation of SHQMM is demonstrated using a quantum transport system as an illustrative example. Sec. 5 presents the results of numerical experiments on the SHQMM model, demonstrating its adaptability on both quantum and classical data, better performance on DA, and robust to random initialization. Finally, in Sec. 6, we summarize our work and provide some insights for future research.

2 Hidden quantum Markov model

The Hidden Markov Model (HMM) is a type of probabilistic graph model that describes the evolutionary properties of Markov dynamics. It consists of two important parameters: the transition matrix \mathbf{T} and the observation matrix \mathbf{C} , which are constant matrices. A HMM can be defined as $\lambda = (\mathbf{T}, \mathbf{C}, x_0)$, where x_0 is the initial state vector. The update of the hidden state and the observable results can be obtained from Eq.1, which represents a state-emitting (Moore) hidden Markov model.

$$\begin{aligned} x_{t+\Delta t} &= \mathbf{T}x_t \\ y_{t+\Delta t} &= \text{diag}(\mathbf{C}_{(y,:)})x_{t+\Delta t}, \end{aligned} \quad (1)$$

where the variable y represents an output symbol in the observable space O .

A Hierarchical Quantum Markov Model (HQMM) can be defined using a set of parameters $\lambda_Q = (\rho_0, K_y)$, similar to the classical Markov process. Here, ρ_0 corresponds to the initial state vector x_0 of the classical Markov model, and the Kraus operator K_y corresponds to the matrices \mathbf{T} and \mathbf{C} . In comparison to the classical Markov model, the Kraus operator K_y plays a dual role as both the evolution state and the observable output result. It satisfies the condition $\sum_m K_m^\dagger K_m = I$. When the system is measured (assuming the measurement or read-out result is y), the density matrix can be expressed as follows [29]:

$$\rho_y(t + \Delta t) = \frac{\sum_{\omega_y} K_{\omega_y} \rho(t) K_{\omega_y}^\dagger}{\text{Tr}[\sum_{\omega_y} K_{\omega_y} \rho(t) K_{\omega_y}^\dagger]} \quad (2)$$

where ω_y denotes the auxiliary dimension of Kraus operator.

The difference between the HMM and the HQMM is shown in Table.1.

Table 1: The difference between the HMM and the HQMM

| Model | HMM | HQMM |
|-------------------------|-------------------------------------|---|
| State | state vector x | density matrix ρ |
| Transition and Emission | matrix \mathbf{T}, \mathbf{C} | Kraus operators $\{K\}$ |
| Steady State | $x^* = \mathbf{T}x^*$ | $\rho^* = \sum_{\omega_y} K_{\omega_y} \rho^* K_{\omega_y}^\dagger$ |
| Probability | $\text{Idiag}(\mathbf{C}_{(y,:)})x$ | $\text{Tr}(\sum_{\omega_y} K_{\omega_y} \rho K_{\omega_y}^\dagger)$ |

To calculate the parameters $\{K\}$ of the HQMM, Adhikary *et.al.* [29] proposed a maximum likelihood estimation algorithm. This algorithm assumes that a set of observation sequences $y_1, y_2, y_3, \dots, y_T$ is known, and constructs the maximum likelihood function based on this data. This is a particular case where $\omega = 1$:

$$\mathcal{L} = -\ln \text{tr} \left(K_{y_T} \cdots K_{y_2} K_{y_1} \rho_0 K_{y_1}^\dagger K_{y_2}^\dagger \cdots K_{y_T}^\dagger \right). \quad (3)$$

Then the parameter solving problem of the HQMM is transformed into a constrained optimization problem:

$$\begin{aligned} &\text{minimize}_{\{K\}} \quad \mathcal{L}(\{K\}) \\ &\text{subject to} \quad \sum_y K_y^\dagger K_y = I, K_y \in \mathbb{C}^{n \times n}. \end{aligned} \quad (4)$$

Stack K_m by column to form a new matrix $\kappa = [K_1, K_2, \dots, K_m]^T$ with dimension $nm \times n$, the constraint condition in Eq.4 can be rewritten as

$$\kappa^\dagger \kappa = I, \kappa \in \mathbb{C}^{nm \times n}. \quad (5)$$

According to Ref.[29], κ in Eq.5 lies on the Stiefel manifold, and the following gradient descent method can be used to solve Eq.4:

$$\begin{aligned} G &= \frac{\partial \mathcal{L}}{\partial \kappa}, \\ \kappa &= \kappa - \tau \mathbf{U} (I + \frac{\tau}{2} \mathbf{V}^\dagger \mathbf{U})^{-1} \mathbf{V}^\dagger \kappa. \end{aligned} \quad (6)$$

In Eq.6, $\mathbf{U} = [G, \kappa]$, $\mathbf{V} = [\kappa, -G]$, and τ is a positive real number.

3 The quantum conditional master equation

In the real physical world, due to the coupling effect between the quantum system and the environment, the Schrodinger equation is not so practical to describe the open quantum system. The quantum master equation is proposed to describe an open quantum system. For an open quantum system, the Hamiltonian form can be applied as

$$H = H_S + H_E + H'. \quad (7)$$

H_S and H_E represent the Hamiltonians of the quantum system and the environment, respectively. The Hamiltonian H' describes the coupling effect between the quantum system and the environment. In the case of weak coupling between the quantum system and the environment, H' can be treated as a perturbation. Using the expansion of the second-order cumulant, we can obtain a description of the evolution of the reduced density matrix.

$$\begin{aligned} \dot{\rho}(t) &= -i\mathcal{L}\rho(t) \\ &- \int_0^t d\tau \langle \mathcal{L}'(t)\mathcal{G}(t,\tau)\mathcal{L}'(\tau)\mathcal{G}^\dagger(t,\tau) \rangle \rho(t). \end{aligned} \quad (8)$$

Here, the Liouvillian super operator is defined as $\mathcal{L} = [H_S, (\dots)]$, $\mathcal{L}' = [H'_S, (\dots)]$. $\mathcal{G}(t, \tau) = G(t, \tau) \times (\dots) \times G^\dagger(t, \tau)$. $G(t, \tau)$ is the Green's function related to H_S . The reduced density matrix is obtained by partially tracing the density matrix of the composite system, that is, $\rho(t) = \text{Tr}_E[\rho_T(t)]$.

In experiments, measurement results are typically linked to changes in the internal state of a system. Therefore, unlike the method used to derive Eq.8, Li et. al. [35] introduced the "detailed balance" condition to illustrate the relationship among different system states when studying the current (the measurement result) of a quantum transport system. This allowed them to derive the quantum conditional master equation (QCME) in Equation 12 and to obtain some interesting results. By adopting the approach of the QCME described in reference [35] and considering the detailed balance among different system states, the general QCME can be expressed as following when the environment space is divided into different subspaces as shown in Figure 1.

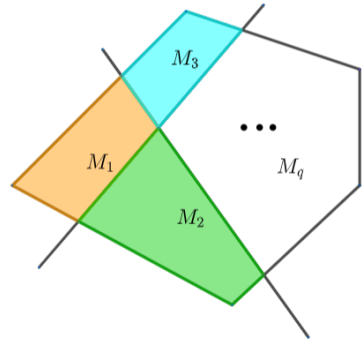


Figure 1: The diagram of dividing the environment space. The Pentagon represents the Hilbert space of the environment, which is divided into some subspace $M_1, M_2, M_3, \dots, M_q$ corresponding to $\rho^{(M_1)}, \rho^{(M_2)}, \dots, \rho^{(M_q)}$.

$$\begin{aligned} \dot{\rho}^{(M_q)} &= -i\mathcal{L}\rho^{(M_q)} \\ &- \int_0^t d\tau \text{Tr}_{E^{(M_q)}}[\mathcal{L}'(t)\mathcal{G}(t,\tau)\mathcal{L}'(\tau)\mathcal{G}^\dagger(t,\tau)\rho_T(t)]. \end{aligned} \quad (9)$$

Here, the proposed initial conditions for the quantum conditional master equation are $\rho_T(0) \simeq \sum_{M_q} \rho^{(M_q)}(0) \otimes \rho_E^{(M_q)}(0)$, and $\rho^{(M_q)}$ denotes *conditional density matrix* of the quantum system corresponding to the environment $\rho_E^{(M_q)}$ associated with the subspace M_q . Note that $\rho^{(M_q)}$ also satisfies positive semi-definite, and $\text{Tr}(\rho^{(M_q)}) \leq 1$, $\text{Tr}[\sum_{M_q} \rho^{(M_q)}] = 1$. The use of quantum conditional master equation enables the representation of the relationship between the different subspaces M_q , which provides a better understanding of the open quantum system being studied.

4 The split hidden quantum Markov model based on QCME

4.1 The quantum master equation of quantum transport system

Since any quantum computing needs an actual physical system to implement, we need search for an open quantum system that can be described by the conditional master equation to establish HQMM. After conducting a search, we found that the quantum transport system is suited for implementing our HQMM based on previous work [29], [35].

As a result, in this section, we present the quantum conditional master equation for the quantum transport system. The Hamiltonian of this quantum system is expressed as follows [35]:

$$H = H_S(a_\mu^\dagger, a_\mu) + \sum_{\alpha=L,R} \sum_{\mu k} \epsilon_{\alpha\mu k} d_{\alpha\mu k}^\dagger d_{\alpha\mu k} + \sum_{\alpha=L,R} \sum_{\mu k} (t_{\alpha\mu k} a_\mu^\dagger d_{\alpha\mu k} + \text{H.c.}) \quad (10)$$

where H_S is the Hamiltonian of the quantum dots system, L and R represent the left and right electrodes respectively, $d_{\alpha\mu k}^\dagger$ and $d_{\alpha\mu k}$ represent the creation and annihilation operators of electrons in the electrode, respectively, and $t_{\alpha\mu k}$ represents the coupling strength between the electrode and the quantum dot system. The master equation for the quantum transport system can be derived through some calculations [35] based on Eq.8:

$$\dot{\rho} = -i\mathcal{L}\rho - \frac{1}{2} \sum_{\mu} \{ [a_\mu^\dagger, A_\mu^{(-)}\rho - \rho A_\mu^{(+)}] + \text{H.c.} \}. \quad (11)$$

If the state space where the electrode is located, without any electrons passing through the quantum dot system, is denoted as $E^{(0)}$, it is formed by the wave function of the two isolated electrodes on the left and right $E^{(0)} = \text{span}\{|\psi_L\rangle \otimes |\psi_R\rangle\}$. If there are n electrons from the state space where the right electrode passes through the quantum dot to the left electrode, it is denoted as $E^{(n)}$ ($n = 1, 2, 3, \dots$). Then the electrode state space E in the equation can be decomposed as $E = \bigoplus_n E^{(n)}$, which leads to the quan-

tum conditional master equation [35] with an initial condition of $\rho_T(0) \simeq \sum_n \rho^{(n)}(0) \otimes \rho_E^{(n)}(0)$.

$$\begin{aligned} \dot{\rho}^{(n)} = & -i\mathcal{L}\rho^{(n)} - \frac{1}{2} \sum_{\mu} \{ [a_\mu^\dagger A_\mu^{(-)}\rho^{(n)} + \rho^{(n)} A_\mu^{(+)} a_\mu^\dagger \\ & - A_{L\mu}^{(-)}\rho^{(n)} a_\mu^\dagger - a_\mu^\dagger \rho^{(n)} A_{L\mu}^{(+)} - A_{R\mu}^{(-)}\rho^{(n-1)} a_\mu^\dagger \\ & - a_\mu^\dagger \rho^{(n+1)} A_{R\mu}^{(+)}] + \text{H.c.} \}. \end{aligned} \quad (12)$$

Here, $\rho^{(n)} = \text{Tr}_{-E^{(n)}}[\rho_T(t)]$ is the conditional density matrix of the quantum dot system [35], which means that there are n electrons passing through the quantum dot system within time t . Here, the number of electrons n corresponds to the subspace \mathcal{M}_q in Eq. 9.

4.2 The relationship between the QCME equation and HQMM

Based on the contents in Sec.3 and 4.1, we derive the hidden quantum Markov model from a quantum master equation and propose a novel stochastic graph model from a quantum conditional master equation. After some calculations (the detailed proof and calculation process are shown in [37]), we obtain:

(1) For quantum master equation of Eq.8, the evolution density matrix of quantum dot system is

$$\rho(t + \Delta t) = \sum_{i,\mu} K_{i,\mu} \rho K_{i,\mu}^\dagger. \quad (13)$$

(2) For quantum conditional master equation of Eq.12, the evolution density matrix of quantum dot system is

$$\rho^{(n)}(t + \Delta t) = \sum_{i,\mu} K_{i,\mu} \rho^{(n)} K_{i,\mu}^\dagger + \sum_{\mu} K_{3,\mu} \rho^{(n-1)} K_{3,\mu}^\dagger + \sum_{\mu} K_{4,\mu} \rho^{(n+1)} K_{4,\mu}^\dagger, \quad (14)$$

where $i = 0, 1, 2$.

Comparing Eq.2($\omega = 1$) and Eq.13, we concluded that there is a close relationship between a quantum Markov model and a quantum master equation. However, the Kraus operators $K_{i,\mu}$ of Eq.14 are involved with the related $\rho^{(n)}$, $\rho^{(n-1)}$, and $\rho^{(n+1)}$. This difference arises from the division of the Hilbert space of the environment, which gives rise to a new HQMM called the split hidden quantum Markov model.

4.3 Split hidden quantum Markov model

In this section, we introduce a SHQMM inspired by a quantum transport system. Similar to the HQMM, the SHQMM is defined by applying a set of parameters $\lambda_{sQ} = (\rho^{(0)}, \rho^{(1)}, \rho^{(2)}, \dots, K_y)$ where $\text{Tr}(\sum_{i=0} K_i) = 1$.

Firstly, the evolution conditional density matrix of quantum system H_S is written as

$$\begin{aligned}\rho^{(\mathcal{M}_q)}(t + \Delta t) &= \sum_y K_y^{(\mathcal{M}_1)} \rho^{(\mathcal{M}_1)}(t) K_y^{(\mathcal{M}_1)\dagger} + \dots \\ &\quad + \sum_y K_y^{(\mathcal{M}_q)} \rho^{(\mathcal{M}_q)}(t) K_y^{(\mathcal{M}_q)\dagger} + \dots,\end{aligned}\quad (15)$$

where, q denotes the values of subspace for environment \mathbf{M} and $\sum_{i,\mu} K_{i,\mu}^\dagger K_{i,\mu} = I$. The parameter y represents the read-out of information symbols from the open quantum system. Eq.15 represents a comprehensive expression that correlates to the relationship between $\rho^{(\mathcal{M}_q)}$.

Secondly, when we read out or measure a certain value y' for $\rho^{(\mathcal{M}_q)}(t)$, the conditional density matrix $\rho^{(\mathcal{M}_q)}(t + \Delta t)$ is rewritten as follows:

$$\begin{aligned}\rho_{y'}^{(\mathcal{M}_q)}(t + \Delta t) &= \frac{\rho_{y'}^{(\mathcal{M}_q)}(t + \Delta t)}{\text{Tr}[\sum_{\mathcal{M}_q} \rho_{y'}^{(\mathcal{M}_q)}(t + \Delta t)]}, \\ \rho_{y'}^{(\mathcal{M}_q)}(t + \Delta t) &= K_{y'}^{(\mathcal{M}_1)} \rho^{(\mathcal{M}_1)}(t) K_{y'}^{(\mathcal{M}_1)\dagger} + \dots \\ &\quad + K_{y'}^{(\mathcal{M}_q)} \rho^{(\mathcal{M}_q)}(t) K_{y'}^{(\mathcal{M}_q)\dagger} + \dots.\end{aligned}\quad (16)$$

Thirdly, the probability of obtaining the measurement result y' is given by:

$$P(y') = \sum_{\mathcal{M}_q} \text{Tr}[\rho_{y'}^{(\mathcal{M}_q)}(t + \Delta t)]. \quad (17)$$

Here, Eq.17 describes the contribution of

$$\begin{aligned}\rho_T^{(0)} &= K_{y_{T-1}} \rho_{T-1}^{(0)} K_{y_{T-1}}^\dagger + A_{y_{T-1}} \rho_{T-1}^{(1)} A_{y_{T-1}}^\dagger, \\ \rho_T^{(1)} &= R_{y_{T-1}} \rho_{T-1}^{(0)} R_{y_{T-1}}^\dagger + K_{y_{T-1}} \rho_{T-1}^{(1)} K_{y_{T-1}}^\dagger + A_{y_{T-1}} \rho_{T-1}^{(2)} A_{y_{T-1}}^\dagger, \\ &\quad \dots \\ \rho_T^{(n)} &= R_{y_{T-1}} \rho_{T-1}^{(n-1)} R_{y_{T-1}}^\dagger + K_{y_{T-1}} \rho_{T-1}^{(n)} K_{y_{T-1}}^\dagger + A_{y_{T-1}} \rho_{T-1}^{(n+1)} A_{y_{T-1}}^\dagger, \\ &\quad \dots \\ \rho_T^{(N_{max})} &= R_{y_{T-1}} \rho_{T-1}^{(N_{max}-1)} R_{y_{T-1}}^\dagger + K_{y_{T-1}} \rho_{T-1}^{(N_{max})} K_{y_{T-1}}^\dagger.\end{aligned}\quad (18)$$

where $K_{i,\mu}$, $K_{3,\mu}$ and $K_{4,\mu}$ of Eq.14 denote K_{y_i} , R_{y_i} and A_{y_i} , respectively. N_{max} denotes the maximum value of n . The probability of y_i is $P(y_i) = \sum_n \text{Tr}[K_{y_i} \rho^{(n)}(t) K_{y_i}^\dagger + R_{y_i} \rho^{(n-1)}(t) R_{y_i}^\dagger + A_{y_i} \rho^{(n+1)}(t) A_{y_i}^\dagger]$.

From Eq.18, the probability of sequences $y_0, y_1 \dots, y_T$ can be easily obtained

different $\rho^{(\mathcal{M}_q)}$ to the probability $P(y')$, and this process reveals the concept of "detailed balance" in physics, as described in Eq.15.

The concretely implement example of our SHQMM To calculate the parameters of the SHQMM, assuming that a set of sequences $y_0, y_1 \dots, y_T$ are known, the conditional density matrix evolution under the measurement result y_i is shown in Fig.2 based on transport system. It can be seen that Fig.2 is similar to a neural network and shows the process of forward propagation through time t . This suggests that SHQMM is promising as a physical realization pathway for QNN, which will be our further research. This demonstrates the connection of quantum state evolution among the different subspaces n in QCME and the conversion relationship among the probabilities $\text{Tr}(\rho^{(n)})$. Compared to previous work on HQMM (the probabilities for the measurement value y_i depend on $\rho = \sum_n \rho^{(n)}$), the property illustrated in Fig.2 also displays the contribution variance of different $\rho^{(n)}$ to the probabilities of obtaining the measurement value y_i at time t_i . Therefore, our model produces a more stable and robust model structure (as seen in experimental results).

Here, based on the QCME (Eq.14), we can write a probability function using the following equations.

$$\begin{aligned}P_{y_0, y_1 \dots, y_T} &= \text{Tr}(\rho_T) \\ \rho_T &= \rho_T^{(0)} + \rho_T^{(1)} + \dots + \rho_T^{(\dots)}.\end{aligned}\quad (19)$$

To compute the parameters of the SHQMM, we propose a maximum likelihood estimation method, based on the results in [26, 29]. Firstly, we use the probability function to derive all pos-

sible Kraus operators, and then use the gradient descent algorithm to find the matrix form of the Kraus operator that satisfies the minimum probability function of the given sequence. This turns parameter-solving into an optimization problem.

$$\begin{aligned} & \text{minimize}_{\{K, R, A\}} \quad \mathcal{L}(\{K, R, A\}) = -\ln \text{Tr}(\rho_T) \\ & \text{subject to} \quad \sum_{y \in O} K_y^\dagger K_y + R_y^\dagger R_y + A_y^\dagger A_y = I. \end{aligned} \quad (20)$$

Stack K_y , R_y , A_y by column to form a new matrix $\kappa = [K_1, K_2, \dots, R_1, R_2, \dots, A_1, A_2, \dots]$ with dimension $3\dim O \cdot m \times m$ (m is the dimension of the Kraus operator). So the constraint condition in Eq.20 can be rewritten as

$$\kappa^\dagger \kappa = I, \kappa \in \mathbb{C}^{3\dim O \cdot m \times m}. \quad (21)$$

We summarize all the above steps into an algorithm for solving the Kraus operator. The specific steps are shown in the Algorithm1.

Algorithm 1 Leaning SHQMM using gradient descent method on Stiefel manifold

Require: Training data $D \in \mathbb{N}^{M \times l}$, W is number of sequences and l is the length of sequence.

Ensure: $\{\mathbf{K}_i\}_{i=1}^{\dim O}$, $\{\mathbf{R}_i\}_{i=1}^{\dim O}$, $\{\mathbf{A}_i\}_{i=1}^{\dim O} \dots$

- 1: **Initialize:** Complex orthogonal matrix on Stiefel $\kappa \in \mathbb{C}^{3\dim O \cdot m \times m}$ and $\rho^{(0)}, \rho^{(1)}, \rho^{(2)}, \dots, \rho^{(N-1)}$ and require that $\rho^{(i)}$ is positive semi-definite and $\sum_{i=0}^{N-1} \rho^{(i)} = \rho_{total}$, ρ_{total} is density matrix.
- 2: **for** $epoch = 1 : E$ **do**
- 3: split the data D into B batches D_B
- 4: **for** $batch = 1 : B$ **do**
- 5: Compute gradient $G_i^{\{K\}} = \frac{\partial \mathcal{L}}{\partial K_i^*}$, $G_i^{\{R\}} = \frac{\partial \mathcal{L}}{\partial R_i^*}$, $G_i^{\{A\}} = \frac{\partial \mathcal{L}}{\partial A_i^*}$
- 6: Compute the like-hood function \mathcal{L}
- 7: Stack $G_i^{\{K\}}$, $G_i^{\{R\}}$, $G_i^{\{A\}}$ vertically to construct $G = [G_1^K, \dots, G_O^A]^T$
- 8: Construct $\mathbf{U} = [G|\kappa]$, $\mathbf{V} = [\kappa|G]$
- 9: $G = \beta G_{old} + (1 - \beta)G$
- 10: Update $\kappa = \kappa - \tau \mathbf{U} (I + \frac{\tau}{2} \mathbf{V}^\dagger \mathbf{U})^{-1} \mathbf{V}^\dagger \kappa$
- 11: **end for**
- 12: Update learning rate $\tau = \alpha \tau$
- 13: **end for**
- 14: Compute the DA function by using the value of probability function \mathcal{L}
- 15: **return** $\{\mathbf{K}_i\}_{i=1}^{\dim O}$, $\{\mathbf{R}_i\}_{i=1}^{\dim O}$, $\{\mathbf{A}_i\}_{i=1}^{\dim O}$ and DA

In Algorithm1, τ (learning rate), α (decay factor) and β (momentum parameter) are the hyper-parameters, and DA is a function that describes the quality of the model. As one of the core evaluation metrics of HQMM, DA [38] is able to measure the performance among models with different structures and functions in a relatively fair way [39], defined as:

$$DA = f\left(1 + \frac{\log \iota P(D|M)}{l}\right). \quad (22)$$

Where, D is data, M is model. l is the length of the sequence, and ι is the number of output symbol in the sequence. The function $f(\cdot)$ is a non-linear segmented function that can map any argument in $(-\infty, 1]$ to $(-1, 1]$, and it is defined as:

$$f(x) = \begin{cases} x, & x \geq 0, \\ \frac{1 - e^{-0.25x}}{1 + e^{-0.25x}}, & x < 0. \end{cases} \quad (23)$$

The model can perfectly predict the Markov sequence if $DA = 1$ and the model better than random model for $DA > 0$.

In the SHQMM, different models can produce different prediction effects for the same sequences, depending on the number $\mathcal{M}q$ of initialized conditional density matrices and the connections between them. Eq.18 describes the closest connection between the conditional density matrix and the number $\mathcal{M}q$, which is equal to n .

During the optimization process, boundary conditions should be considered to avoid situations where the Kraus operators (R , A) converge to zero. The optimal solution of HQMM is one of the optimal solutions of Eq.20. Therefore, periodic boundary conditions are applied to the first and last conditional density matrices, similar to the arrangement of atoms in a crystal.

$$\begin{aligned} \rho_T^{(0)} &= K_{y_{T-1}} \rho_{T-1}^{(0)} K_{y_{T-1}}^\dagger + A_{y_{T-1}} \rho_{T-1}^{(1)} A_{y_{T-1}}^\dagger \\ &+ R_{y_{T-1}} \rho_{T-1}^{(N_{max})} R_{y_{T-1}}^\dagger, \\ \rho_T^{(N_{max})} &= R_{y_{T-1}} \rho_{T-1}^{(N_{max}-1)} R_{y_{T-1}}^\dagger + K_{y_{T-1}} \rho_{T-1}^{(N_{max})} K_{y_{T-1}}^\dagger \\ &+ A_{y_{T-1}} \rho_{T-1}^{(0)} A_{y_{T-1}}^\dagger. \end{aligned} \quad (24)$$

Different from Eq.18, Eq.24 includes periodic boundary conditions to circumvent instances where the Kraus operators (R , A) converge to zero.

More detailed cases are presented in [37].

Extend the expandability ability of the SHQMM If we need to further improve the complexity of the model, we can set the parameters $N_{max} = 4, 5, 6, \dots$ and apply a more complicated connection defined as k -local. Thus, the general SHQMM can be defined as a tuple $\lambda_{SQ} = (\mathbb{C}^m, k\text{-local}, K_y^j, y \in O, j = 2k + 1, \rho_0^{(i)}, i \in [0, N_{max} - 1])$ with the following conditions:

(1) $\rho_0^{(i)}$ is conditional density matrix, $\text{Tr}(\sum_{i=0}^{N_{max}-1} \rho_0^{(i)}) = 1$.

(2) For every Kraus operator, $K_y^j : \mathbb{C}^m \rightarrow \mathbb{C}^m$ and $\sum_{y,j} (K_y^j)^\dagger K_y^j = I$.

(3) The evolution of $\rho^{(i)}$ follows Eq.25.

$$\rho^{(i)}(t + \Delta t) = \sum_{j'=-\lfloor \frac{j}{2} \rfloor}^{\lfloor \frac{j}{2} \rfloor} \sum_{y \in O} K_y^{j'+1+\lfloor \frac{j}{2} \rfloor} \rho^{(i-j')}(t) K_y^{j'+1+\lfloor \frac{j}{2} \rfloor \dagger}, \quad (25)$$

where the periodic boundary conditions should be applied and conditional density matrix beyond index range should be zeroed, that is, $0 \leq i - j' \leq N_{max} - 1$. $\lfloor \frac{j}{2} \rfloor$ equal to k , $j' \in \{-\lfloor \frac{j}{2} \rfloor, -\lfloor \frac{j}{2} \rfloor + 1, \dots, \lfloor \frac{j}{2} \rfloor - 1, \lfloor \frac{j}{2} \rfloor\}$.

(4) The probability of observation symbol y is

$$p(y) = \sum_{i=0}^{N-1} \text{Tr} \left(\sum_{j'=-\lfloor \frac{j}{2} \rfloor}^{\lfloor \frac{j}{2} \rfloor} K_y^{j'+1+\lfloor \frac{j}{2} \rfloor} \rho^{(i-j')}(t) K_y^{j'+1+\lfloor \frac{j}{2} \rfloor \dagger} \right), \quad (26)$$

where, k -local represents the relationship between different conditional density matrix and j represents the number of Kraus operator classes.

In summary, strengthening state correlations and transitioning from basic neighbor connections can improve the usability of SHQMM for various time series problems..

Comparison of properties of SHQMM and HQMM We use a simple case to illustrate the correlation and difference between SHQMM and HQMM. For 1-local model, by summing the conditional density matrix $\rho^{(n)}$ with index n in Eq.18, we obtain:

$$\begin{aligned} \rho(t + \Delta t) &= \sum_y K_y \rho(t) K_y^\dagger + \sum_y R_y \rho(t) R_y^\dagger \\ &+ \sum_y A_y \rho(t) A_y^\dagger \\ &= \sum_{\omega_y} K_{\omega_y} \rho(t) K_{\omega_y}^\dagger. \end{aligned} \quad (27)$$

The second equal sign in Eq.27 shows a formal relationship between SHQMM and HQMM, but our model has clear physical implications compared to the auxiliary dimension ω_y in Eq.2 (HQMM with $\omega = 3$). This indicates that the SHQMM is a valid HQMM at the same time. The differences between SHQMM and HQMM lie in the following aspects:

- SHQMM makes density matrix have a hierarchy structure as shown in Fig.2, and the density matrix evolves through multiple channels.
- Kraus operator $\{K_y^j\}_{y \in O}^{j=2k+1}$ acts on different conditional density matrix $\rho^{(n)}$ in SHQMM, whereas in HQMM, Kraus operator $\{K_{\omega_y}\}_{y \in O}$ acts on total density matrix ρ .
- SHQMM can be derived from actual physical systems, such as quantum transport systems, as shown in Fig.2.

The SHQMM can reflect the relationship between hidden states and is more suitable for handling more complex data than the HQMM. From a physical system implementation point of view, the quantum conditional master equation may differ from the quantum transport system for other open quantum systems[31, 32, 33], resulting in different split hidden quantum Markov models. The Bayesian rule for SHQMM is:

$$\rho_{y|x}^{(n)}(t + \Delta t) = \frac{\sum_{j'=\lfloor \frac{j}{2} \rfloor}^{\lfloor \frac{j}{2} \rfloor} K_y^{j'+1+\lfloor \frac{j}{2} \rfloor} \rho^{(n-j')}(t) K_y^{j'+1+\lfloor \frac{j}{2} \rfloor \dagger}}{\text{Tr} \left(\sum_{n=0}^{N-1} \sum_{j'=\lfloor \frac{j}{2} \rfloor}^{\lfloor \frac{j}{2} \rfloor} K_y^{j'+1+\lfloor \frac{j}{2} \rfloor} \rho^{(n-j')}(t) K_y^{j'+1+\lfloor \frac{j}{2} \rfloor \dagger} \right)}. \quad (28)$$

Eq.28 expresses, under the principle of conditional probability, the quantum state corresponding to the system when the system is observed as x at t and as y at $t + \Delta t$. Table 2 shows the properties of the SHQMM and HQMM.

5 Experiment and results

In this section, we applied quantum and classical data to train and test our SHQMM. All experiments were performed on an experimental platform outfitted with Intel Core i7 CPU and 16 GB RAM, trials were executed on Python 3.8 with PyTorch and qiskit libraries for modeling and evaluating. The source code and further details are available at [here](#).

Quantum data Firstly, we used the quantum data generated by a quantum mechanical process in Ref.[26]. The quantum data has six hidden states and six observational values. The size of the quantum data is 40×3000 .

Training and validation We use 20×3000 data to train our model, generating a total of 20 models. Simultaneously, we used 10×3000 data to verify the model, and the remaining data were used to test the model. The results are shown in Fig.3 with hyperparameters $\tau = 0.95, \alpha = 0.95, \beta = 0.90$ (More calculation results can be found in [37]). Fig.3 shows several models λ_{SQ} for single, double and three qubits quantum system which are used to construct the SHQMM under the different parameters N and k . It found : (1) With the increase of the qubit number, the value of DA also increases and reaches a stable value at about 20 epochs (three qubits exceed 20 epochs). (2) Apart from the single bit, the connection mode (different k-local) and N have little effect on the DA value. (3) While a higher number of quantum bits results in a relatively larger value of DA, the standard deviation (STD) decreases as the number of qubits increases during evaluation with alternative data. This suggesting potential overfitting.

To further test the reliability of our model, we will evaluate it from several perspectives.

Initialize Kraus In Ref. [29], it was stated that the training outcome of HQMM is susceptible to the initial Kraus operators in smaller models. Thus, this study investigates the effect of the initial position of Kraus operators on Stiefel manifolds for SHQMM. Eq. 29 is utilized to evaluate the distance between various initial positions.

$$D(\kappa_1, \kappa_2) = \|\kappa_1 \kappa_2^\dagger - I\|_2. \quad (29)$$

When $\kappa_1 = \kappa_2$, $D = 0$. The initialization method for the Kraus operator is presented in Algorithm 2. The varying behaviors of the DA are depicted in Figure 4 for different random initialization seeds (RS). Results clearly shows that our proposed SHQMM remains stable regardless of the initial Kraus values, thus confirming its validity.

Algorithm 2 Initial Kraus operator on Stiefel manifolds

Require: the dimension of Kraus operator m , the class of Kraus operator j , the dimension of observable space $\text{dim}O$ and random seed RS

Ensure: Kraus operator $\{K_y^j\}$

- 1: **Initialize:** random vector $\vec{v}_1 = \text{random}(m \cdot j \cdot \text{dim}O, 1, \text{RS})$, zero matrix $\kappa = \text{zeros}(m \cdot j \cdot \text{dim}O, 2m)$, $\kappa(:, 1) = \frac{\vec{v}_1}{\|\vec{v}_1\|}$
- 2: **for** $s = 2 : 2m$ **do**
- 3: $\vec{v}_s = \text{random}(m \cdot j \cdot \text{dim}O, 1)$
- 4: **if** all column vectors in κ and \vec{v}_s are orthogonal **do**
- 5: $\vec{v}_s = \frac{\vec{v}_s}{\|\vec{v}_s\|}$; $\kappa(:, s) = \vec{v}_s$
- 6: **else do**
- 7: Schmidt Orthogonalization of κ and \vec{v}_s
- 8: $\vec{v}_s = \frac{\vec{v}_s}{\|\vec{v}_s\|}$; $\kappa(:, s) = \vec{v}_s$
- 9: **end if**
- 10: **end for**
- 11: construct new matrix $\kappa' = \kappa(:, 1 : m) / \sqrt{2} + \kappa(:, m + 1 : 2m) / \sqrt{2}$
- 12: split κ' into Kraus operator

Table 2: The properties of HQMM and sHQMM

| Model | State | Transition and Emission | Probability | Bayesian Rule | Evolution |
|-------|------------------------------|------------------------------------|--|--------------------|---|
| SHQMM | $\{\rho^{(i)}\}_{i=0}^{N-1}$ | quantum channel \mathcal{K}_s | Eq.26 | $\rho_{y x}^{(n)}$ | Eq.25 |
| HQMM | ρ | quantum channel \mathcal{K} | $\text{Tr}(\sum_{\omega_y} K_{\omega_y} \rho(t) K_{\omega_y}^\dagger)$ | Eq.2 | $\sum_{\omega_y} K_{\omega_y} \rho(t) K_{\omega_y}^\dagger$ |

Selection of effective models Given the various methods available to construct models, selecting the most effective one for a given dataset is a critical challenge. Typically, the expressiveness of a model is directly linked to the number of its parameters. The number of parameters for SHQMM is as follows:

$$\mathcal{N}_P = m^2 \cdot j. \quad (30)$$

The corresponding results are shown in Fig.5 to obtain best training results, we should change the dimension m of Kraus operator firstly and then adjust the parameter j for a given sequence.

Hyperparameters selection for the model To obtain the optimal DA , Algorithm 1 employs three hyperparameters, namely τ , α , and β . Fig. 6 demonstrates the impact of varying hyperparameters on DA , indicating that DA is more sensitive to changes in α as compared to τ . Moreover, the existence of multiple local optima in SHQMM is evident. To identify the global optimum, we investigated the effect of momentum parameter β on DA for the best case ($\tau = 0.95, \alpha = 0.95$) and the worst case ($\tau = 0.65, \alpha = 0.65$), as presented in Fig.7. It was observed that DA may reach the global optimum at $\tau = 0.95, \alpha = 0.95$, and $\beta = 0.90$, and that DA can be further enhanced by selecting a different β . However, after computing the distance of Kraus solutions between different hyperparameters ($\tau = 0.95, \alpha = 0.95, \beta = 0.90$ and $\tau = 0.65, \alpha = 0.65, \beta = 0.60$) using Eq. 29, we discovered that their DA values were comparable despite locating at different positions on the Stiefel manifold.

Classical data To conduct a thorough evaluation of the model, classical data generated by a hidden Markov process with transition matrix

\mathbf{T} and emission matrix \mathbf{C} were utilized to compute the Kraus operator and determine DA . The results obtained from the classical data are presented in Fig. 8, where hyperparameters were set to $\tau = 0.95$, $\alpha = 0.95$, and $\beta = 0.90$.

Similar to the quantum case, the value of DA also increases and reaches a stable state after approximately 20 epochs (for three qubits, it took 20 epochs to stabilize). The different values of k -local have little impact on the DA value, and the standard deviation (STD) continues to decrease as the qubit number increases for the testing data, possibly due to model overfitting. Additional test results can be found in [37].

$$\mathbf{T} = \begin{pmatrix} 0.8 & 0.01 & 0 & 0.1 & 0.3 & 0 \\ 0.02 & 0.02 & 0.1 & 0.15 & 0.05 & 0 \\ 0.08 & 0.03 & 0.1 & 0.4 & 0.05 & 0.5 \\ 0.05 & 0.04 & 0.5 & 0.35 & 0 & 0.5 \\ 0.03 & 0.5 & 0.03 & 0 & 0.6 & 0 \\ 0.02 & 0.4 & 0.27 & 0 & 0 & 0 \end{pmatrix},$$

$$\mathbf{C} = \begin{pmatrix} 0.2 & 0 & 0.05 & 0.95 & 0.01 & 0.05 \\ 0.7 & 0.1 & 0.05 & 0.01 & 0.05 & 0.05 \\ 0.05 & 0.8 & 0.1 & 0.02 & 0.05 & 0.04 \\ 0.04 & 0.04 & 0.02 & 0 & 0.84 & 0.11 \\ 0.01 & 0.03 & 0.7 & 0.01 & 0.02 & 0.2 \\ 0 & 0.03 & 0.08 & 0.01 & 0.03 & 0.55 \end{pmatrix}.$$

Result

- For our data, as the number of qubits increases, the DA of the model shows that the best promotion rates (from one qubit to three qubits) are 72.04%(quantum data) and 73.40%(classical data), but they are highly over-fitting. The possible reason is that the model is too complex for the simple data.
- As the number of qubits increases and hyperparameters remain constant, the training step converges more slowly.

- SHQMM is stable for different sequences, $STD(DA) < 0.01$
- The SHQMM is robust to the initial value of the Kraus operator that may be the reason for the hierarchy structure of conditional density matrix.

6 Conclusion

In this paper, we first investigate the hidden quantum Markov process using quantum conditional master equations, and in this way propose a new stochastic probabilistic graphical model SHQMM. On the learning problem of the HQMM model, the paper proposes a new algorithm to realize the model parameter update, in particular the generation of the Krauss operator, which is restricted to the Stiefel manifold. Numerical experiments on SHQMM show that the model has a better performance on DA than previous models, and is more insensitive to the initial state with higher robustness. Through the analysis, SHQMM can be used to explain the closer relationship between the hidden states of quantum systems associated with time series data. Therefore, SHQMM can be used as a new tool for understanding open quantum systems and solving time series problems in machine learning. The model has a correspondence with quantum transport systems, so the model has good prospects for physical implementation. Due to the similarity of its structure, SHQMM can also serve as an important theoretical basis for the physical realization of QNN.

7 Acknowledgements

This work is supported by the National Key R&D Program of China, Grant No.2018FYA0306703 and Chengdu Innovation and Technology Project, No.2021-YF05-02413-GX and 2021-YF09-00114-GX, the Open Fund of Advanced Cryptography and System Security Key Laboratory of Sichuan Province (Grant No. SKLACSS-202210), Sichuan Province key research and development project, No.2022YFG0315.

References

- [1] Paul Benioff. “The computer as a physical system: A microscopic quantum mechanical Hamiltonian model of computers as represented by Turing machines”. *Journal of statistical physics* **22**, 563–591 (1980).
- [2] Richard P Feynman. “Simulating physics with computers”. *Int. J. Theor. Phys.* **21** (1982).
- [3] Juan I Cirac and Peter Zoller. “Quantum computations with cold trapped ions”. *Physical review letters* **74**, 4091 (1995).
- [4] IH Deutsch, GK Brennen, and PS Jessen. “Special Issue on Physical Implementations of Quantum Computing”. *Fortschr. Physik (Progress of Physics)* **48**, 925 (2000).
- [5] Emanuel Knill, Raymond Laflamme, and Gerald J Milburn. “A scheme for efficient quantum computation with linear optics”. *nature* **409**, 46–52 (2001).
- [6] Nicola Pancotti, Patrick Rebentrost, Nathan Wiebe, Jacob Biamonte, Peter Wittek, and Seth Lloyd. “Quantum machine learning”. *Nature* **549**, 195–202 (2017).
- [7] M Cerezo, Guillaume Verdon, Hsin-Yuan Huang, Lukasz Cincio, and Patrick J Coles. “Challenges and opportunities in quantum machine learning”. *Nature Computational Science* **2**, 567–576 (2022). [arXiv:10.1038/s43588-022-00311-3](https://arxiv.org/abs/10.1038/s43588-022-00311-3).
- [8] Thi Ha Kyaw, Tobias Haug et.al., Kishor Bharti, Alba Cervera-Lierta. “Noisy intermediate-scale quantum (NISQ) algorithms” (2021). [arXiv:2101.08448v1](https://arxiv.org/abs/2101.08448v1).
- [9] Alán Aspuru-Guzik, Roland Lindh, and Markus Reiher. “The matter simulation (r) evolution”. *ACS central science* **4**, 144–152 (2018).
- [10] Iulia M Georgescu, Sahel Ashhab, and Franco Nori. “Quantum simulation”. *Reviews of Modern Physics* **86**, 153 (2014).
- [11] Markus Reiher, Nathan Wiebe, Krysta M Svore, Dave Wecker, and Matthias Troyer. “Elucidating reaction mechanisms on quantum computers”. *Proceedings of the National Academy of Sciences* **114**, 7555–7560 (2017).

[12] Yudong Cao, Jhonathan Romero, and Alán Aspuru-Guzik. “Potential of quantum computing for drug discovery”. *IBM Journal of Research and Development* **62**, 6–1 (2018).

[13] Roman Orus, Samuel Mugel, and Enrique Lizaso. “Quantum computing for finance: Overview and prospects”. *Reviews in Physics* **4**, 100028 (2019).

[14] Pierre-Luc Dallaire-Demers, Jonathan Romero, Libor Veis, Sukin Sim, and Alán Aspuru-Guzik. “Low-depth circuit ansatz for preparing correlated fermionic states on a quantum computer”. *Quantum Science and Technology* **4**, 045005 (2019).

[15] Elizabeth Fons, Paula Dawson, Jeffrey Yau, Xiao-jun Zeng, and John Keane. “A novel dynamic asset allocation system using Feature Saliency Hidden Markov models for smart beta investing”. *Expert Systems with Applications* **163**, 113720 (2021).

[16] PV Chandrika, K Visalakshmi, and K Sathi Srinivasan. “Application of Hidden Markov Models in Stock Trading”. In 2020 6th International Conference on Advanced Computing and Communication Systems (ICACCS). Pages 1144–1147. (2020). [arXiv:10.1109/ICACCS48705.2020.9074387](https://arxiv.org/abs/10.1109/ICACCS48705.2020.9074387).

[17] Dima Suleiman, Arafat Awajan, and Wael Al Etaiwi. “The use of hidden Markov model in natural arabic language processing: A survey”. *Procedia computer science* **113**, 240–247 (2017).

[18] Hariz Zakka Muhammad, Muhammad Nasrun, Casi Setianingsih, and Muhammad Ary Murti. “Speech recognition for English to Indonesian translator using hidden Markov model”. In 2018 International Conference on Signals and Systems (ICSigSys). Pages 255–260. IEEE (2018).

[19] Erik LL Sonnhammer, Gunnar Von Heijne, Anders Krogh, et al. “A hidden Markov model for predicting transmembrane helices in protein sequences”. In LSMB 1998. Pages 175–182. (1998). url: <https://cdn.aaai.org/ISMB/1998/ISMB98-021.pdf>.

[20] Gary Xie and Jeanne M Fair. “Hidden Markov Model: a shortest unique representative approach to detect the protein toxins, virulence factors and antibiotic resistance genes”. *BMC Research Notes* **14**, 1–5 (2021).

[21] Sean R Eddy. “What is a hidden markov model?”. *Nature biotechnology* **22**, 1315–1316 (2004). [arXiv:10.1038/nbt1004-1315](https://arxiv.org/abs/10.1038/nbt1004-1315).

[22] Paul M Baggenstoss. “A modified baum-welch algorithm for hidden markov models with multiple observation spaces”. *IEEE Transactions on speech and audio processing* **9**, 411–416 (2001). [arXiv:10.1109/89.917686](https://arxiv.org/abs/10.1109/89.917686).

[23] Aleksandar Kavcic and Jose MF Moura. “The viterbi algorithm and markov noise memory”. *IEEE Transactions on information theory* **46**, 291–301 (2000). [arXiv:10.1109/18.817531](https://arxiv.org/abs/10.1109/18.817531).

[24] Todd K Moon. “The expectation-maximization algorithm”. *IEEE Signal processing magazine* **13**, 47–60 (1996). [arXiv:10.1109/79.543975](https://arxiv.org/abs/10.1109/79.543975).

[25] Alex Monras, Almut Beige, and Karoline Wiesner. “Hidden quantum Markov models and non-adaptive read-out of many-body states” (2010). [arXiv:1002.2337](https://arxiv.org/abs/1002.2337).

[26] Siddarth Srinivasan, Geoff Gordon, and Byron Boots. “Learning hidden quantum markov models”. In Amos Storkey and Fernando Perez-Cruz, editors, *Proceedings of the Twenty-First International Conference on Artificial Intelligence and Statistics*. Volume 84 of *Proceedings of Machine Learning Research*, pages 1979–1987. PMLR (2018). url: <https://proceedings.mlr.press/v84/srinivasan18a.html>.

[27] Herbert Jaeger. “Observable operator models for discrete stochastic time series”. *Neural computation* **12**, 1371–1398 (2000).

[28] Qing Liu, Thomas J. Elliott, Felix C. Binder, Carlo Di Franco, and Mile Gu. “Optimal stochastic modeling with unitary quantum dynamics”. *Phys. Rev. A* **99**, 062110 (2019).

[29] Sandesh Adhikary, Siddarth Srinivasan, Geoff Gordon, and Byron Boots. “Expressiveness and Learning of Hidden Quantum Markov Models”. In *International Conference on Artificial Intelligence and Statistics*. Pages 4151–4161. (2020). url: <http://proceedings.mlr.press/v108/adhikary20a/adhikary20a.pdf>.

[30] Bo Jiang and Yu-Hong Dai. “A framework of constraint preserving update schemes for optimization on Stiefel manifold”. *Mathematical Programming* **153**, 535–575 (2015).

[31] Yoshitaka Tanimura. “Stochastic Liouville, Langevin, Fokker–Planck, and master equation approaches to quantum dissipative systems”. *Journal of the Physical Society of Japan* **75**, 082001 (2006).

[32] Akihito Ishizaki and Graham R Fleming. “Unified treatment of quantum coherent and incoherent hopping dynamics in electronic energy transfer: Reduced hierarchy equation approach”. *The Journal of chemical physics* **130** (2009).

[33] Jinshuang Jin, Xiao Zheng, and YiJing Yan. “Exact dynamics of dissipative electronic systems and quantum transport: Hierarchical equations of motion approach”. *The Journal of chemical physics* **128** (2008).

[34] Daniel A. Roberts and Sho Yaida. “The Principles of Deep Learning Theory” (2021). [arXiv:2106.10165v1](https://arxiv.org/abs/2106.10165v1).

[35] Xin-Qi Li, JunYan Luo, Yong-Gang Yang, Ping Cui, and YiJing Yan. “Quantum master-equation approach to quantum transport through mesoscopic systems”. *Physical Review B* **71**, 205304 (2005).

[36] Lewis A Clark, Wei Huang, Thomas M Barlow, and Almut Beige. “Hidden quantum markov models and open quantum systems with instantaneous feedback”. In *ISCS 2014 Interdisciplinary Symposium on Complex Systems*. Pages 143–151. (2015). [arXiv:10.1007/978-3-319-10759-2_16](https://arxiv.org/abs/10.1007/978-3-319-10759-2_16).

[37] Author. “Please see Supplemental Material accompanying the manuscript for computational methods and additional results”. - - - (2023).

[38] Ming-Jie Zhao and Herbert Jaeger. “Norm-observable operator models”. *Neural computation* **22**, 1927–1959 (2010). [arXiv:10.1162/neco.2010.03-09-983](https://arxiv.org/abs/10.1162/neco.2010.03-09-983).

[39] Sandesh Adhikary, Siddarth Srinivasan, and Byron Boots. “Learning quantum graphical models using constrained gradient descent on the stiefel manifold” (2019). [arXiv:2101.08448v1](https://arxiv.org/abs/2101.08448v1).

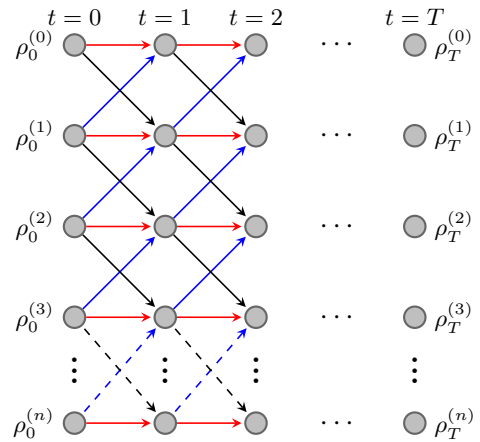


Figure 2: The expanded calculation diagram of $\rho^n(t)$ for a set of sequences $y_0, y_1 \dots, y_T$: The red line represents the Kraus operator K_y in $\{K\}$, the black line represents the Kraus operator R_y in $\{R\}$, and the blue line represents the Kraus operator A_y in $\{A\}$

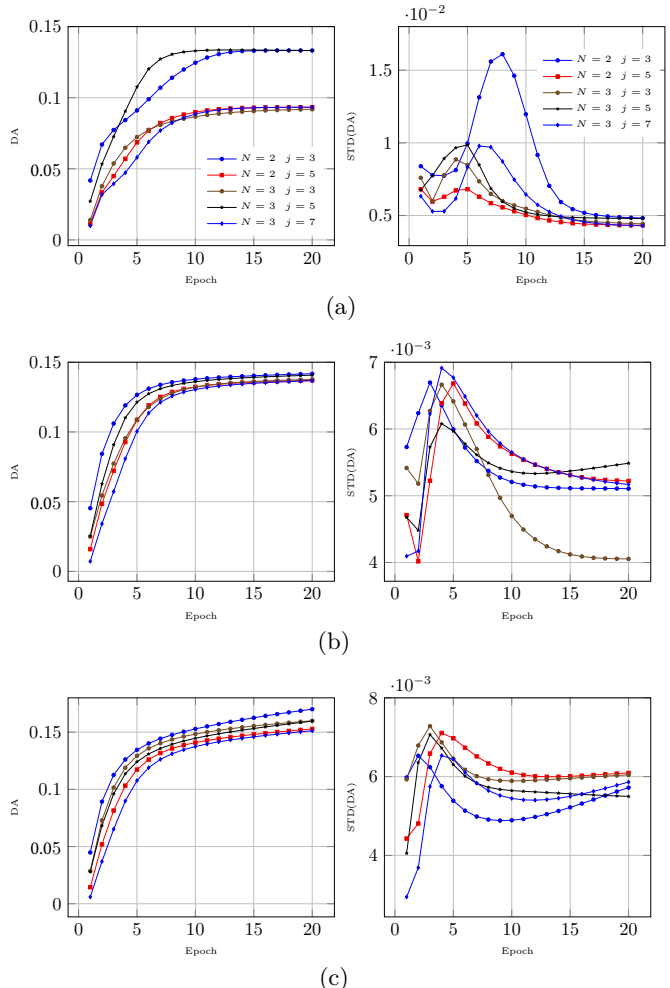


Figure 3: The training result of the different SHQMM for quantum data under different parameters N and $j = 2k + 1$. The subfigures (a), (b), (c) represent the training results for choosing single, double and three qubits quantum system, respectively.

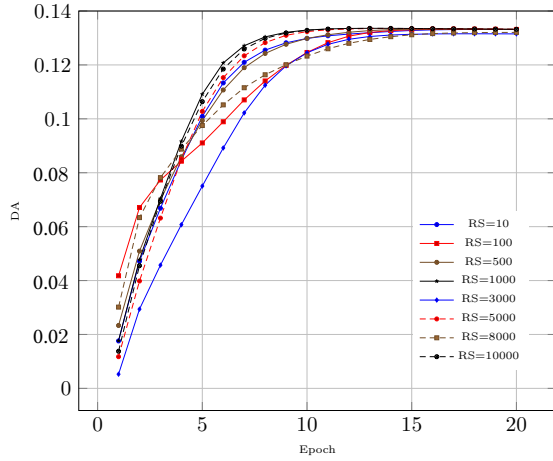


Figure 4: The training result of SHQMM($N_{max} = 3$, AR, Single Qubit) in random initialization

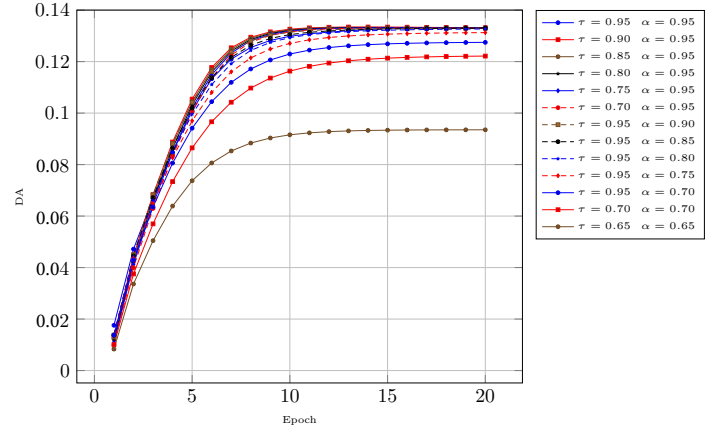
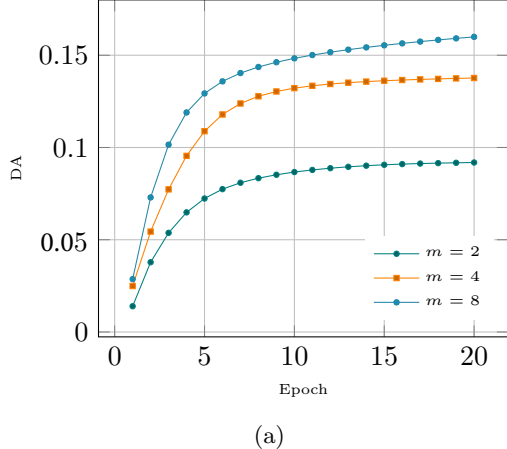
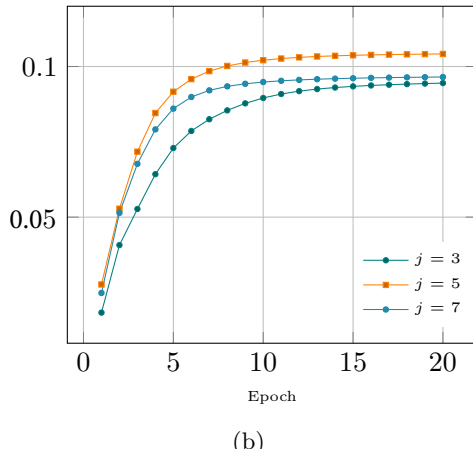


Figure 6: The effect of DA on different hyperparameters tuple(τ, α)($\beta = 0.90$). The best DA is 0.1332($\tau = 0.95, \alpha = 0.95$) and the worst DA is 0.0951($\tau = 0.65, \alpha = 0.65$)

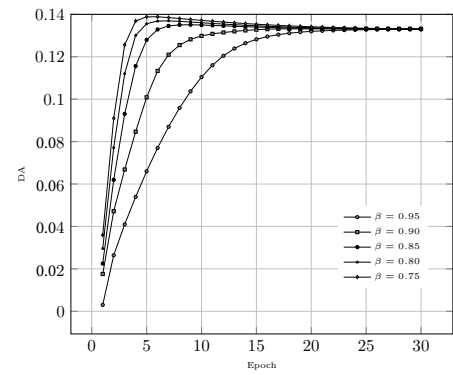


(a)

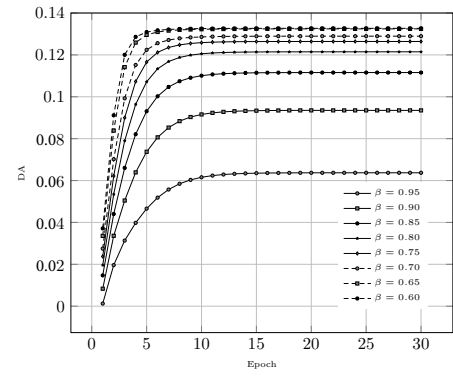


(b)

Figure 5: The relationship between the training outcome of SHQMM and the number of parameters. (a) represents the variation of DA with the dimension m of the Kraus operator. (b) represents the variation of DA with the j of the conditional density matrix. The training results are more sensitive to m than j

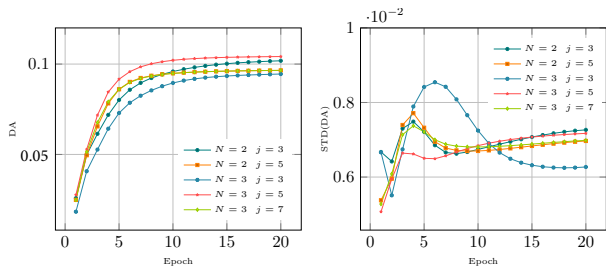


(a)

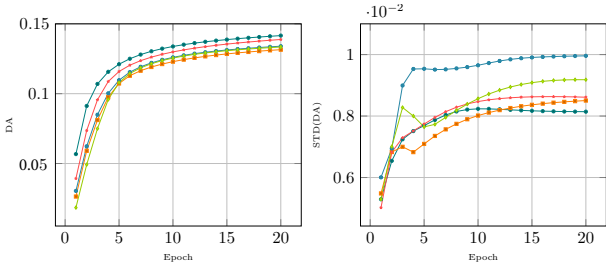


(b)

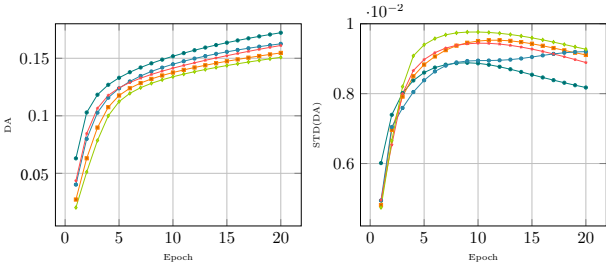
Figure 7: Choose the hyperparameters for sHQMM. (a) shows the DA of $\tau = 0.95, \alpha = 0.95$; (b) shows the DA of $\tau = 0.65, \alpha = 0.65$.



(a)



(b)



(c)

Figure 8: The training results of SHQMM for classical data under different parameters N and $j = 2k + 1$. The subfigures (a), (b), (c) represent the training results for choosing single, double and three qubits quantum system, respectively.